Indian Journal of Chemical Technology
Vol. 29, May 2022, pp. 288-295

Enhanced catalytic and biological activities of Cu doped ZnO nanoparticles synthesized by microwave assisted method

Saranya Rishikesan[1, 2] Mubarak Ali Muhamath Basha*[,3] , Jeyalakshmi Kumaramangalam[4] & M Sherin Banu[5]

[1]Centre for Research and Evaluation, Bharathiar University, Coimbatore 641 046, Tamilnadu, India.

[2]Department of Chemistry, Annai Women's College, Karur 639136, Tamil Nadu, India.

[3]Department of Chemistry, Chikkaiah Naicker College, Erode 638 004, Tamil Nadu, India.

[4]Department of Chemistry, M.Kumarasamy College of Engineering, Karur 639 113, Tamilnadu, India.

[5]Department of Chemistry, Government Arts College (A), Salem 636 007, Tamilnadu, India.

E-mail: masterscience2003@yahoo.co.in

Received 2 July 2021; accepted 6 April 2022

Copper doped zinc oxide nanoparticles (Cu-ZnO Nps) are known to be one of the multifunctional inorganic materials with effective antibacterial activity. In the present study, un-doped and copper doped zinc oxide with varying concentration i.e., Zn_{1-x} Cu_xO (where x = 0, 0.01, 0.02 and 0.03%) have been synthesized via microwave assisted method and characterized by XRD, SEM, EDAX, TEM, UV-VIS-DRS spectroscopy. X-ray diffraction studies show that the Cu-ZnO Nps exhibit hexagonal wurtzite structure and the particle size are found to be within the range between 20 to 35 nm. Cu-ZnO Nps exhibit appreciable catalytic activity (89.9% yields) in the transformation of benzylalcohol to benzaldehyde. Significant antibacterial activity is shown by Cu-ZnO Nps against bacterial strains such as *E. coli, S. aureus, Klebsiella* and *B. subtilis* with zone of inhibition of 15 ± 0.08, 17 ± 0.21, 21 ± 0.01 and 23 ± 0.69 mm respectively in contrast to standard antibiotic streptomycin. The *in vitro* cytotoxicity of ZnO and Cu-ZnO Nps has been determined against human breast (MCF7) and human cervical (HeLa) cancer cell lines using MTT assay.

Keywords: Antibacterial, Anticancer activity, Catalytic activity, Cu-ZnO Nps, Microwave assisted method

Morphology-controlled fabrication of nanostructures has become one of the most important and challenging aspects in the field of modern nanotechnology due to their potential applications in biological, magnetic, optical, electronic and mechanical nanodevices[1, 2]. Metal oxide nanoparticles, specifically nano-structured ZnO, have gained considerable importance in recent years due to their wide range of applications in various fields of science notably biotechnology and pharmacology[3]. ZnO nanoparticles have been regarded as biocidal agents/disinfectants because of their safety, lower toxicity and biocompatibility towards humans[4]. However, doping of transition metal (TM) into ZnO structure leads to modification in the physical properties like crystal size, dislocation density, bond length and lattice strain etc[5,6]. There are numerous synthetic methods available for the preparation of pure and doped ZnO nanomaterials, like hydrothermal, hydrolysis, sol-gel, vapor condensation, spray pyrolysis and organic precursor flame decomposition[7]. In conventional synthesis, energy is transferred to the material through convection, conduction and radiation, which results in temperature gradient between surface and bulk. Compare to other methods, microwave synthesis is a relatively new chemical method to facilitate reactions and could be another avenue for green synthesis of nanomaterials. Several attributes of microwave heating contribute to greener syntheses, including shorter reaction time, lower energy consumption and higher product yield[8]. The microwave heating causes uniform distribution of temperature between the surface and the bulk material and thereby leading to the fast formation of nanoparticles. The microwave dielectric heating has resulted in acceleration of the chemical transformations in a microwave field, which cannot be achieved easily by the conventional method[9,10].

Due to the outbreak of the infectious diseases caused by different pathogenic bacteria, the scientists are searching for new antibacterial agents[11]. Among metal oxide Nps, ZnO are comparatively inexpensive, relatively less toxic and also exhibit excellent biomedical applications[12]. Antimicrobial activity of ZnO has enhanced due to the presence of water molecules on its surface, these aqueous suspensions

of ZnO and water generate free radicals of hydroxyl and oxygen species which is responsible for remarkable oxidative stress in treated bacterial cells. Currently prototype ZnO Nps are used as delivering systems for vaccines and anti-cancer drugs[13]. The functionality and efficiency of ZnO nanostructures can be improved by increasing and modifying their surface area by adding some dopant materials i.e. biomolecules and transition metals (Mn, Fe, Cr, Cu) at nanoscale[14]. Through surface modification with transition metals, ZnO nanoparticles could be used as biosensors, antimicrobial, antioxidants, drug delivery systems and bio-imaging materials[15].

Comparably to the other transition metals, Cu is preferred for doping of ZnO due to its similar electronic shell structure, physical and chemical properties as those of Zn[16]. Based on the existing literature, we can presume that Cu substituted ZnO Nps are an alternative solution for killing bacterial as well as cancer cells[17]. Especially, Cu is considered as one of the most effective doping elements for improving the anticancer activity of ZnO Nps. In our previous work, the inherent selective cytotoxicity of ZnO Nps against human breast cancer cells (MCF7) and human cervical carcinoma (HeLa) can be improved by doping of Cu^{2+} ion[18]. Cu substitution in ZnO plays multiple roles in enhancing the interfacial charge transfer, defect chemistry, ROS generation, and bacterial inhibition. Therefore, these features make Cu substitution in ZnO more suitable for biological applications such as bacterial and cancer treatment which are hardly explored[19]. The present work reveals the microwave assisted technique for synthesis of Cu doped ZnO Nps. The synthesized samples were characterized by XRD, EDAX, SEM, TEM and UV-VIS-DRS spectroscopy techniques and its catalytic, antibacterial and anticancer activities were investigated.

Experimental Section

Synthesis of Nanoparticles

Pure and Cu doped ZnO with compositional formula $Zn_{1-x}Cu_xO$ (x = 0.00, 0.01, 0.02 and 0.03) were synthesized by microwave assisted method. 8 mL of 0.6 M urea was added drop wise into the 6 mL of 0.4 M zinc nitrate ($ZnNO_3 \cdot 6H_2O$) solution under continuous stirring. Copper nitrate ($CuNO_3 \cdot 2H_2O$) solution was added in required quantity according to the compositional formula. Zinc nitrate and copper nitrate solution together with urea (fuel) were placed inside a home-based convection microwave oven (Brand - IFB; Model - 20SC2) then subjected to microwave energy for 10 min at 1200 Watts and microwave frequency of 2450 MHz. After microwave processing, the solution was cooled to room temperature. The resulted precipitate was separated by centrifugation, then washed with deionized water and ethanol for several times, finally the precipitate was dried in an oven at 80°C for 24 h and calcinated at 400°C for 1 h. ZnO nanoparticles were also prepared by the same procedure without the addition of copper nitrate. The synthesized samples were designated as ZnO (a), Cu doped in 0.01% as (b), 0.02% as (c) and 0.03% as (d).

Characterization

The X-Ray diffraction patterns of ZnO and Cu-ZnO samples have been recorded by X-ray diffractometer from Rigaku by using Cu-Kα radiation. Average crystallite size was calculated by measuring the full width at the half maximum (FWHM) by using Debye-Scherrer equation[20]

$$L = \frac{0.89\,\lambda}{\beta \cos \theta} \quad \ldots(1)$$

where, L = average crystallite size (Å), λ = wavelength of the incident X-ray beam (1.54 Å), β = FWHM (rad), and θ = Bragg's angle. High resolution scanning electron microscopy (HR-SEM) images have been acquired from Philips XL30 ESEM fitted alongside energy dispersive X-ray spectroscopy. High resolution transmission electron microscopy (HR-TEM) images was recorded on Philips EM 208 transmission electron microscope using 200 kV accelerating voltage. Cary 100 UV-visible spectrophotometer was used to record diffuse reflectance spectra for the samples.

Catalytic tests

In order to investigate the catalytic activity of pure and Cu-doped ZnO, the oxidation of benzyl alcohol have studied by altering the reaction conditions with the effect of the oxidant (H_2O_2) and solvent (acetonitrile). The samples were heated at 80 °C in acetonitrile medium for 8 h in a three necked round bottom flask, equipped with a reflux condenser and thermometer. After the catalytic reaction, the oxidized products were collected and analyzed using Agilent GC spectrometer. The column used for this study was DB wax column (capillary column) of length 30 mm and helium was used as the carrier gas.

Antibacterial tests

To investigate the antibacterial ability, the samples were tested against four bacterial strains namely

E. coli, *S. aureus*, *Klebsiella* and *B. subtilis*. The samples were dissolved in dimethyl sulphoxide and it was made into the required concentrations. The bacterial strains were inoculated separately in 25 mL of nutrient broth in a conical flask and incubated for 24 h to get active strain by using well diffusion method. Muller Hinton agar was poured separately into petri-dishes. After solidification of 0.25 mL of test strains were inoculated in the media separately and care was taken to ensure proper homogenization. The experiment was performed under strict aseptic conditions. After the medium solidified, a well was made in the plates with sterile borer (5mm). 25 µL of the test sample was introduced into the well and plates were incubated at 37°C for 72 h. All samples were tested in triplicates. Microbial growth was determined by measuring the diameter of zone of inhibition. The standard antibiotic streptomycin was used as a control for antibacterial assay.

In vitro cytotoxicity evaluation by MTT assay

MCF7 and HeLa cells were grown in Eagle's minimum essential medium containing 10% fetal bovine serum (FBS). 100 µL per well of cell suspension were seeded into 96-well plates at plating density of 10,000 cells/well and incubated to allow for cell attachment at 37 °C, 5% CO_2, 95% air and 100% relative humidity. After 24 h the cells were treated with various concentrations such as 12.5, 25, 50, 100 and 200 µg/mL of ZnO, Cu-ZnO samples. Triplication was maintained, and the medium without the test sample served as the control. After 24 h, the wells were treated with 20 µL MTT [5 mg mL^{-1} phosphate buffered saline (PBS)] and incubated at 37 °C for 4 h. The medium with MTT was then removed separately and the formed formazan crystals were dissolved in 100 mL DMSO. The graph was plotted between the percentage of cell inhibition and the concentration of the samples. IC_{50} values were calculated from the percentage of inhibition. The percentage of cell inhibition was determined using the formula, % inhibition = [mean OD of untreated cells (control)/mean OD of treated cells (control)] ×100.

Results and Discussion

XRD analysis

Figure 1 depicted the XRD pattern of the $Zn_{1-x}Cu_xO$ samples with various concentration of Cu (0.00, 0.01, 0.02 and 0.03). The obtained XRD diffraction peaks appeared at 31.0, 37.0, 44.5, 56.0, 59.5 and 65.5. These peaks can be assigned to the preferred orientation of

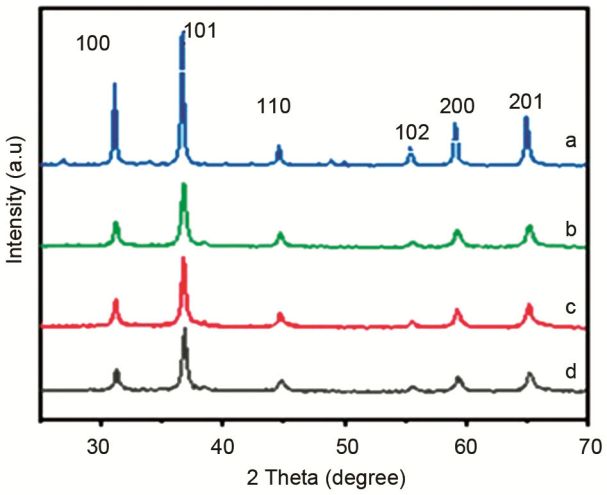

Fig.1 — XRD pattern of (a) ZnO; (b) ZnO-$Cu_{0.01\%}$; (c) ZnO-$Cu_{0.02\%}$ and (d) ZnO-$Cu_{0.03\%}$

(100), (101), (110), (102), (200) and (201) of the hexagonal structure of ZnO and Cu-ZnO Nps. The diffraction peaks of the material agreed well with the diffraction data from the JCPDS file number (06-2151) and no characteristic peaks were observed other than ZnO. This indicates that Cu^{2+} ion successfully occupy the lattice site rather than interstitial one. This is due to the fact that ionic radius of Cu^{2+} (0.73Å) is very close to that of Zn^{2+} (0.74Å), due to which Cu can easily penetrate into ZnO crystal lattice. Literature showed that the trace of the samples of copper doping possessed wurtzite structure while those with higher copper concentration CuO starts to form cluster and is isolated as impurity phase[21]. The highest peak obtained in the XRD spectra (101) plane was the preferential plane of orientation.

The sharp and intensive diffraction peaks indicated that the products were well crystallized. In addition, decrease in the peak intensity and broadening of the peak width was observed. This was due to the formation of particles with smaller average diameters as a result of increase in lattice disorder upon Cu^{2+} ions substitution. The average crystallite size was calculated from Debye-Scherrer formula. It was originated to be 31.98, 28.43, 24.12 and 21.76 nm correspond to Cu concentration of 0.00, 0.01, 0.02 and 0.03% respectively. The results indicated that the average crystallite size tends to decrease with increasing Cu concentrations. The average crystallite size of Cu-ZnO Nps has been observed to be smaller than that of ZnO. This was due to the presence of Cu^{2+} ions in the ZnO lattice which prohibited the growth of crystal grains.

Morphological analysis

Surface morphologies of ZnO and Cu-ZnO Nps have been examined by using SEM and TEM analysis. Figures 2(a-d) shows representative SEM images of Cu-ZnO Nps (x = 0, 0.01, 0.02, and 0.03). The images suggested that the average size of the materials were in the range of nanometer. These images showed the presence of large aggregates of smaller individual nanoparticles of various sizes. Figure 2(a) showed that the un-doped ZnO Nps were homogeneous in nature and equally distributed over the surface. On the other hand, Fig. 2 (b-d) showed that the shape of the doped particles changed from spheroid to rod-like. The average size of the particles observed by SEM was below 100 nm, which was consistent with the XRD results.

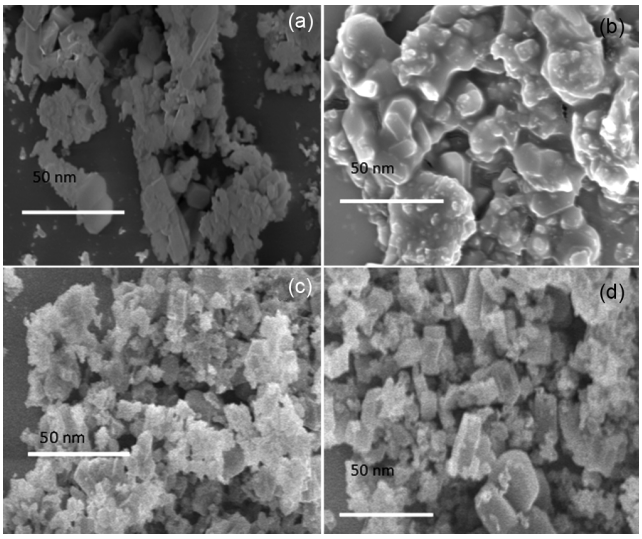

Fig. 2 — SEM image of (a) ZnO; (b) ZnO-$Cu_{0.01\%}$; (c) ZnO-$Cu_{0.02\%}$ and (d) ZnO-$Cu_{0.03\%}$

The SEM results showed that size and shape of the ZnO Nps is depended on Cu dopant concentration. Most of the grains tend to be in a shape of hexagonal. Agglomeration takes place among the particles which might be as a consequence of interaction of dipole-dipole between the particles. The grain size was measured by employing a method of line intercepts that usually situated in the middle of 19 nm and 29 nm. The average grain size slightly tends to decrease with increase in Cu doping. This tendency was also observed in the XRD measurements.

The elemental compositions of ZnO and Cu-ZnO Nps were investigated by EDAX spectra and shown in Fig. 3(a-d). The EDAX spectra showed signals of all the expected elements Zn, O and Cu, which confirmed the presence of Cu^{2+} ions which were substituting the Zn^{2+} ions in the Zn matrix. Hence, these results concluded that Cu ions have been doped into the ZnO lattice without any other elemental impurities present in the prepared samples. The EDAX peak positions were consistent with ZnO, and the sharp peaks of EDAX indicated that the materials

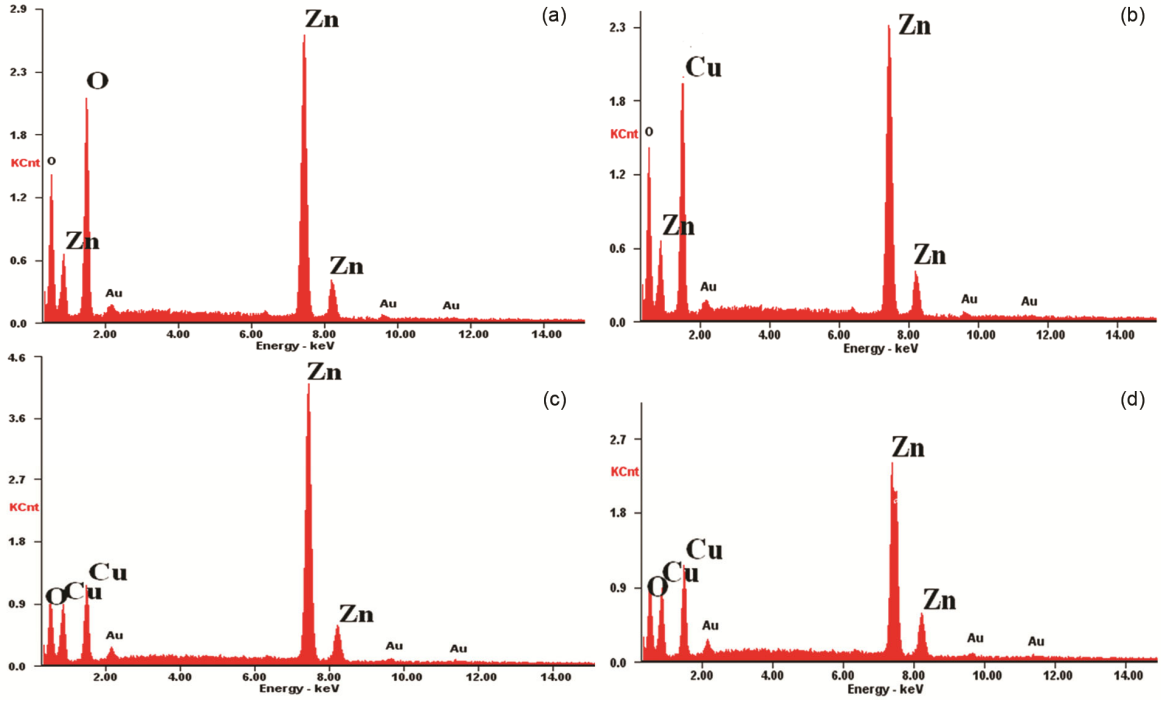

Fig. 3 — EDAX spectra of (a) ZnO; (b) ZnO-$Cu_{0.01\%}$; (c) ZnO-$Cu_{0.02\%}$ and (d) ZnO-$Cu_{0.03\%}$

had crystalline structures[22]. The strong intensity and narrow width of ZnO diffraction peaks indicate that the resultant products were highly crystalline in nature. These findings were in close agreement with previous reports[23].

The corresponding TEM images of Cu-ZnO Nps (x = 0.01, 0.02, and 0.03) were shown in Figs 4(a–d). From TEM images, we observed consistent particles distribution which have distinguishable boundaries on grain. The particles get agglomerated similar to a chain, and also every particle displays a structure of ball-shaped granular. The size of the particles observed in the TEM image was in the range of 20-35 nm. This was in good agreement with that estimated by Debye - Scherrer's formula from the XRD pattern.

Diffuse reflectance spectroscopic studies

The diffuse reflectance UV-Visible spectra were recorded between the wavelength regions starting from 350 to 800 nm for synthesized samples (Fig. 5). UV-visible spectra of Cu-ZnO materials exhibited a wide shoulder peak in the wavelength region 350 to 375 nm which was due to some structural defects. The shoulder peak intensity decreases on increasing Cu content which indicated that the minimization of growth of crystallite as well as structural defects[24, 25].

Catalytic studies

The catalytic activity of Cu-ZnO Nps was studied for the oxidation reaction of benzyl alcohol in the presence of oxidant H_2O_2 using acetonitrile medium. In many instances, benzyl alcohol oxidation selectively oxidizes directly into benzaldehyde. Likewise, benzaldehyde was a major oxidation product through the current research study. With respect to the similar reaction condition, blank reactions were carried out without any oxidant and catalyst which exhibited minimal yield of around 3.5 % only. The reaction was also executed with catalyst alone (without oxidant), the yield obtained was 7.8% whereas the reaction with oxidant (without catalyst) ended up with only 28.2 % yield. This clearly proved that the oxidant (H_2O_2) alone was not able to oxidize benzyl alcohol directly into benzaldehyde. The reaction was optimized with oxidant concentration and the synthesized materials were used as catalysts. The reaction with highest dopant concentration (0.03%) of Cu-ZnO Nps showed 89.90% yield of benzaldehyde (Table 1).

Antibacterial activity

The antibacterial activity of ZnO and Cu doped ZnO Nps was investigated against *Echerichia coli (E.coli), Staphylococcus aureus (S. aureus), Klebsiella* and *Bacillus Subtilis (B. subtilis*). The antimicrobial activity of ZnO and Cu-ZnO Nps was being exploited by mixing with wound dressing materials. The growth behavior of bacterial species in the presence of the prepared samples has been studied via OD method[26]. The results of the experiments were obtained by the measuring the zone of inhibition. Figure 6 represents the growth curvatures of *E. coli, S. aureus, Klebsiella, B. subtilis* were treated with the ZnO and Cu doped ZnO Nps in three various concentrations such as 25, 50 and 75 µg/mL). The

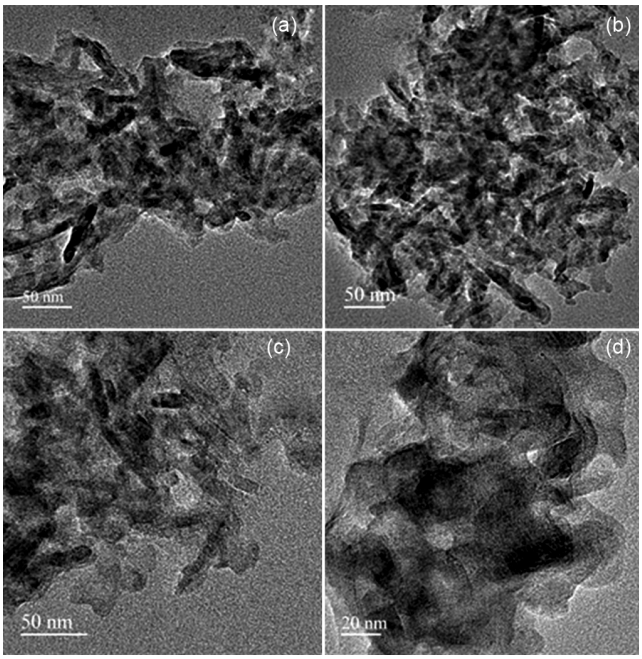

Fig. 4 — TEM image of (a) ZnO; (b) ZnO-$Cu_{0.01\%}$; (c) ZnO-$Cu_{0.02\%}$ and (d) ZnO-$Cu_{0.03\%}$

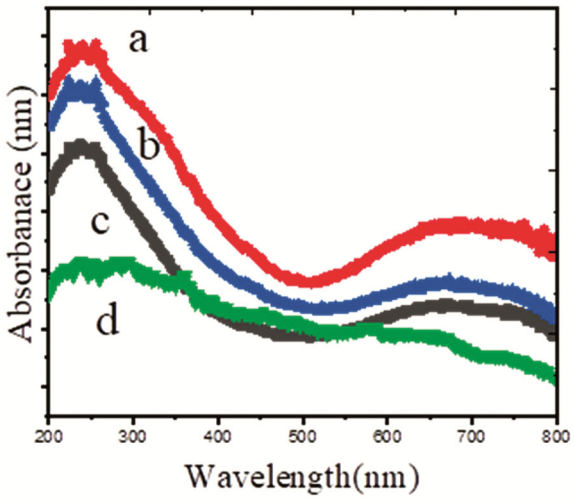

Fig. 5 — DRS Spectra of (a) ZnO; (b) ZnO-$Cu_{0.01\%}$; (c) ZnO-$Cu_{0.02\%}$ and (d) ZnO-$Cu_{0.03\%}$

Table 1 — Catalytic performance of ZnO and Cu-ZnO Nps in the presence of H_2O_2 oxidant in the conversion of benzyl alcohol to benzaldehyde

S.No	Catalyst used	Amount of the catalyst (g)	Oxidant	Reaction time(h)	Yield (%)
1		0	-	8	3.5
2	ZnO	0.5	-	8	7.8
3	-	0	H_2O_2	8	28.2
4	ZnO	0.5	H_2O_2	8	55.32
5	$Cu_{0.01\%}$ - ZnO	0.5	H_2O_2	8	65.3
6	$Cu_{0.02\%}$ - ZnO	0.5	H_2O_2	8	78.4
7	$Cu_{0.03\%}$ - ZnO	0.5	H_2O_2	8	89.9

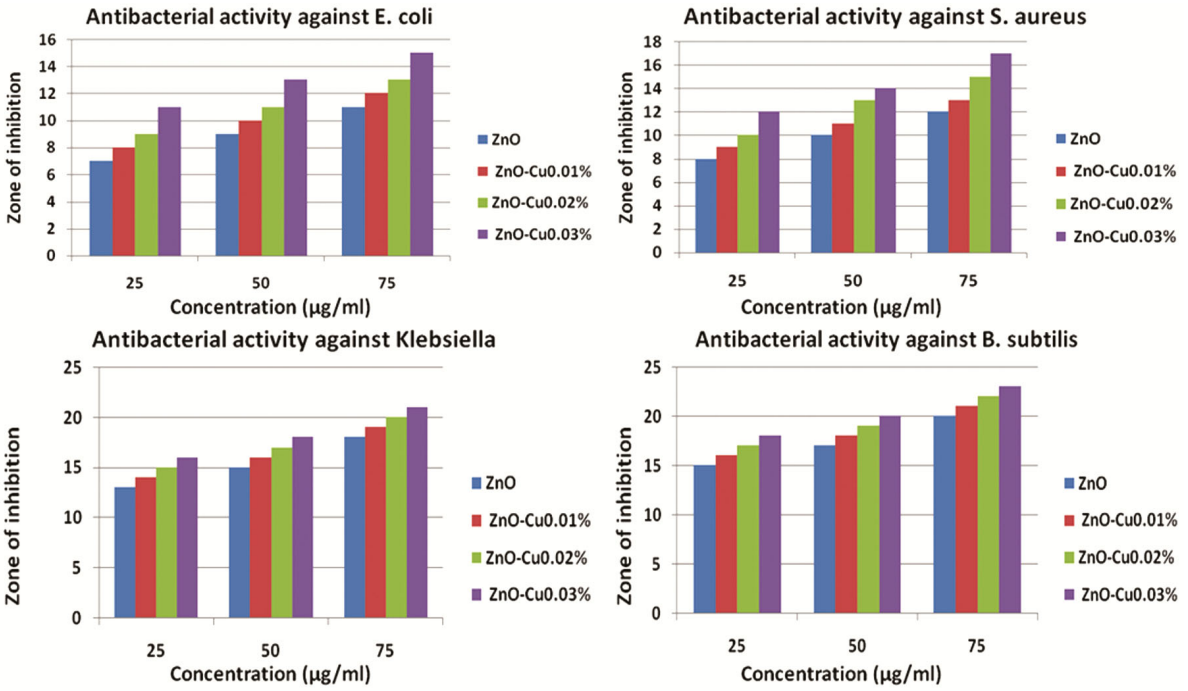

Fig. 6 — Antibacterial activity of ZnO and Cu-ZnO Nps

results (Table 2) revealed that the ZnO Nps with higher dopant concentration (ZnO-$Cu_{0.03\%}$) showed the effective antibacterial activity against all the above mentioned bacterial strains in a dose dependent manner. Prominent activity of ZnO-$Cu_{0.03\%}$ was observed against *Klebsiella* and *B. subtilis* with zone of inhibition (ZOI) of 21 ± 0.01 mm and 23 ± 0.69 mm respectively. The obtained ZOI were compared with streptomycin as standard drug. It is worth mention that the ZnO and Cu-ZnO Nps showed comparable and even better activity than streptomycin. The important observation from the antibacterial studies was that the activity increases with dopant concentration.

The superior antibacterial activity of Cu doped ZnO Nps was due to the fact that the copper ions released from Cu-doped ZnO nanoparticles permeated and destroyed the bacterial cell membrane structure by attaching to the negatively-charged cell wall[27]. Copper ions and zinc ions were involved in cross-linkage of nucleic acid strands by binding them with DNA molecule of bacteria. This results in a disordered helical structure of DNA molecule which causes denaturation of proteins and other biochemical processes in the cell, leading to complete destruction of the bacterial cell[28]. Factors which affect the sensitivity of bacteria to Cu-doped ZnO Nps were size of particles, temperature of synthesis, structure of bacterial cell wall, and degree of contact of the Nps with bacteria[29-32].

Anticancer activity

The *in vitro* cytotoxic activity of the compound was determined against human breast (MCF7), human cervical (HeLa) cancer cell lines using MTT assay.

Table 2 — Antibacterial activity of ZnO and Cu-ZnO nanoparticles

Bacterial strains	Concentration (µg/mL)	Zone of inhibition (mm)				
		ZnO	$Cu_{0.01\%}$ - ZnO	$Cu_{0.02\%}$ - ZnO	$Cu_{0.03\%}$ - ZnO	Standard Antibiotic Streptomycin
E. coli	25	07 ± 0.04	08 ± 0.08	09 ± 0.05	11 ± 0.10	11 ± 0.09
	50	09 ± 0.03	10 ± 0.10	11 ± 0.23	13 ± 0.04	12 ± 0.03
	75	11 ± 0.09	12 ± 0.05	13 ± 0.01	15 ± 0.08	13 ± 0.14
S. aureus	25	08 ± 0.02	09 ± 0.10	10 ± 0.04	12 ± 0.30	12 ± 0.05
	50	10 ± 0.14	11 ± 0.13	13 ± 0.20	14 ± 0.90	13 ± 0.56
	75	12 ± 0.07	13 ± 0.12	15 ± 0.17	17 ± 0.21	14 ± 0.78
Klebsiella	25	13 ± 0.10	14 ± 0.05	15 ± 0.08	16 ± 0.90	13 ± 0.04
	50	15 ± 0.09	16 ± 0.07	17 ± 0.03	18 ± 0.11	14 ± 0.17
	75	18 ± 0.85	19 ± 0.05	20 ± 0.03	21 ± 0.01	15 ± 0.96
B. subtilis	25	15 ± 0.06	16 ± 0.10	17 ± 0.43	18 ± 0.85	14 ± 0.09
	50	17 ± 0.25	18 ± 0.69	19 ± 0.71	20 ± 0.37	15 ± 0.38
	75	20 ± 0.56	21 ± 0.78	22 ± 0.95	23 ± 0.69	16 ± 0.87

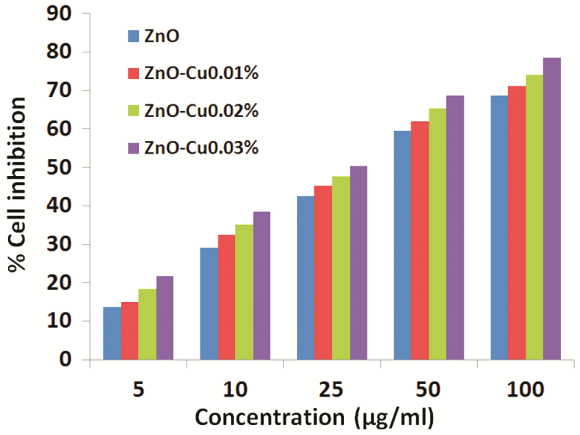

Fig. 7a — *In vitro* anticancer activity of Cu-ZnO against MCF7 cell line

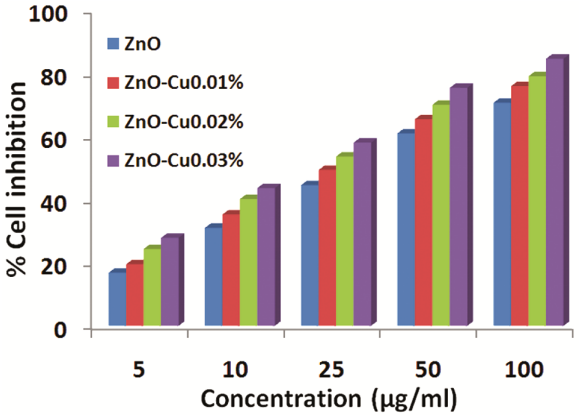

Fig. 7b — *In vitro* anticancer activity of Cu-ZnO against HeLa cell line

The cytotoxicity of ZnO and Cu-ZnO Nps after 24 h incubation against MCF7 and HeLa cell lines is shown in Figs 7a and 7b. The results were analyzed by means of cell inhibition expressed as IC_{50} values

Table 3 — Anticancer activity of ZnO and Cu-ZnO Nps against MCF7 & HeLa Cancer cell lines

Nanoparticles	IC_{50} (µg/mL)	
	MCF7	HeLa
ZnO	35	31
$Cu_{0.01\%}$ - ZnO	30	24
$Cu_{0.02\%}$ - ZnO	25	19
$Cu_{0.03\%}$ - ZnO	21	15

(Table 3). All the synthesized materials showed anticancer activity against MCF7 and HeLa cell lines with IC_{50} value ranging from 15-35 µg/mL. Comparatively, higher activity was exhibited by ZnO-$Cu_{0.03\%}$ with IC_{50} value of 21 µg/mL and 15µg/mL against MCF7 and HeLa cell lines respectively. From the investigation, it is showed that the Cu doped ZnO Nps showed enhanced activity than ZnO Nps. Typically, small sized particles play a significant role in the death of cancer cells as Cu-ZnO Nps was small than undoped ZnO Nps. There were evidences which showed doping enhanced the anticancer activity[33].

Conclusion

In conclusion, pure ZnO and Cu doped with ZnO have been synthesized by simple and eco-friendly microwave assisted method. Doping effect on the particle size, crystallinity, catalysis and biological properties of the Cu-ZnO Nps were observed. The hexagonal wurtzite morphology of ZnO and Cu-ZnO Nps was confirmed by XRD analyses. TEM and SEM examination presented the formation of Zn and Cu-ZnO Nps within the nanoscale range of 20-50 nm. Cu-ZnO Nps with higher dopant (0.03%) concentration acted as efficient catalyst for the conversion of benzylalcohol to benzaldehyde and

similarly it exhibited significant antibacterial activity against bacterial strains such as *E. coli, S. aureus, Klebsiella* and *B. subtilis* with zone of inhibition of 15 ± 0.08, 17 ± 0.21, 21 ± 0.01 and 23 ± 0.69 mm respectively. The activity obtained was comparable with standard antibiotic streptomycin. Cu-ZnO Nps (ZnO-$Cu_{0.03\%}$) exhibited potent anticancer activity against MCF7 and HeLa cancer cell lines with the IC_{50} values of 21µg/mL and 15µg/mL respectively. From the investigation it was concluded that the Cu-ZnO Nps with higher dopant concentration showed enhanced catalytic, antibacterial and anticancer activity than ZnO Nps.

Acknowledgements

One of the authors thank Dr. R. Karvembu, Professor, Department of Chemistry, National Institute of Technology, Tiruchirappalli for providing the lab facility.

Compliance with ethical standards

Conflict of interest There are no conflicts to declare.

Ethical approval This article does not contain any studies involving animals.

References

1 Sayed M A E, *Acc Chem Res*, 34 (2001) 257.
2 Xia Y, Yang P, Sun Y, Wu Y, Mayers B, Gates B, Yin Y, Kim F & Yan H, *Adv Mater*, 15 (2003) 353.
3 Javed R, Usman M, Tabassum S & Zia M, *Appl Surf Sci*, 386 (2016) 319.
4 Bogutska K I, Sklyarov Y P & Prylutskyy Y I, *Ukrainica Bioorganica Acta*, 1 (2013) 9.
5 Singhal S, Kaur J, Namgyal T & Sharma R, *Physica B*, 407 (2012) 1223.
6 Das T, Das B K, Parashar K, Kumar R, Choudhary H K, Anupama A V, Sahoo B, Sahoo P K & Parashar S K S, *J Mater Sci Mater Electron*, 28 (2017) 13587.
7 Djerdj I, Zvonko J, Denis A & Markus N, *Nanoscale*, 2 (2010) 1096.
8 Zhu Y J & Chen F, *Chem Rev*, 114 (2014) 6462.
9 Sharma D, Sharma S, Kaith B S, Rajput J & Kaur M, *Appl Surf Sci*, 257 (2011) 9661.
10 Hamedani N F, Mahjoub A R, Khodadadi A A & Mortazavi Y, *Sens Actuators B Chem*, 156 (2011) 737.
11 Badhusha M S M, *Der Pharma Chemica*, 8 (2016) 78.
12 Jiang J, Pi J & Cai J, *Bioinorg Chem Appl*, 2018 (2018) 1.
13 Reddy K M, Feris K, Bell J, Wingett D G, Hanley C & Punnoose A, *Appl Phys Lett*, 90 (2007) 213902.
14 Abdollahi Y, Abdullah A H, Zainal Z, Yusof N A, *Int J Basic Appl Sci*, 11 (2011) 62.
15 Rezapour M & Talebian N, *Mater Chem Phys*, 129 (2011) 249.
16 Ashokkumar M & Muthukumaran S, *J Lumin*, 162 (2015) 97.
17 Gupta J & Bahadur D, *ACS Sust Chem Eng*, 5 (2017) 8702.
18 Saranya R & Mubarak Ali M, *Acta Chim Slov*, 67 (2020) 235.
19 Fu M, Li Y, Wu S, Lu P, Liu J & Dong F, *Appl Surf Sci*, 258 (2011) 1587.
20 Becheri A, Durr M, Nostro P L & Baglioni P, *J Nanopart Res*, 10 (2008) 679.
21 Kelsall R W, Hamley I W & Geoghegan M, *Nanoscale Sci Technol*, (John Wiley & Sons) (2006).
22 Ghaffarian H R, Saiedi M, Sayyadnejad M A & Rashidi A M, *Iran J Chem Chem Eng*, 30 (2011) 1.
23 Ong C H & Gong H, *Thin Solid Films*, 445 (2003) 299.
24 Ng Y C, Shamsuddin M, *J Iran Chem Soc*, 8 (2011) 28.
25 Ragupathia C, Vijaya J J, Kennedy L J & Bououdina M, *Ceram Inter*, 40 (2014) 13067.
26 Sawai J & Yoshikawa T, *J Appl Microbiol*, 96 (2004) 803.
27 Ijaz F, Shahid S, Khan S A, Ahmad W & Zaman S, *Trop J Pharm Res*, 16 (2017) 743.
28 Khan S A, Noreen F, Kanwal S, Iqbal A & Hussain G, *Mater Sci Eng C*, 28 (2018) 46.
29 Khan S A, Kanwal S, Iqbal A & Ahmad W, *Int J Adv Res*, 5 (2017) 1350.
30 Khan S A, Shahid S, Sajid M R, Noreen F & Kanwal S, *Int J Adv Res*, 5 (2017) 925.
31 Hussain G, Khan S A, Ahmad W, Athar M & Saleem R, *Int J Adv Res*, 5 (2017) 234.
32 Fakhroueian Z, Dehshiri A M, Katouzian F & Esmaeilzadeh P, *J Nanopart Res*, 16 (2014) 2483.
33 Carofiglio M, Barui S, Cauda V & Laurenti M, *Appl Sci*, 10 (2020) 5194.